Construction and Building Materials 432 (2024) 136657

Contents lists available at ScienceDirect

Construction and Building Materials

journal homepage: www.elsevier.com/locate/conbuildmat

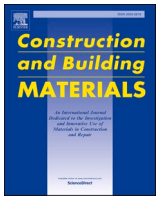

Experimental and operations viability assessment of powder-to-powder (P2P) mixture of graphene and cement for industrial applications

Akilu Yunusa-Kaltungo [a,*], Meini Su [a], Patrick Manu [d], Clara M. Cheung [a], Alejandro Gallego-Schmid [a], Raphael Ricardo Zepon Tarpani [a], Jingyue Hao [b], Lin Ma [c]

[a] Department of Mechanical, Aerospace and Civil Engineering (MACE), University of Manchester, M13 9PL, UK
[b] Department of Earth and Environmental Sciences, University of Manchester, M13 9PL, UK
[c] Department of Chemical Engineering, University of Manchester, M13 9PL, UK
[d] School of Architecture and Environment, University of the West of England, Frenchay Campus, Coldharbour Lane, Bristol BS16 1QY, UK

ARTICLE INFO

Keywords:
Sustainability
Energy reduction
Graphene-cement
Powder-to-powder
Occupational safety and health
Cost and benefits analysis

ABSTRACT

Studies have demonstrated that a minute quantity of graphene is sufficient to boost cement characteristics, but the attainment of good dispersion and uniformity of the resultant graphene-cement mixture remains a challenge. To alleviate these challenges, this study proposes a low-energy powder-to-powder homogeniser for dispersing reasonably large quantities of graphene powder into cement powders. Microscopic analysis of graphene dispersion from two samples (1% and 0.02% graphene) at 5x, 10x and 20x objectives revealed that graphene accounts for 1.3% and 0.09% over the cement area respectively, which is relatively uniform across all selected samples. Furthermore, four different dosages of graphene were used to validate the impacts of various proportions of graphene, i.e., 0%, 0.02%, 0.04% and 0.06% (by mass of cement) on two types of cement (i.e., Portland cement CEM I 52.5 N and Portland cement CEM II 42.5 N) which also revealed compressive strength increases up to 25% at 7 and 28 days.

1. Introduction

Concrete is universally regarded as the most consumed man-made material on earth [1]. The inherent benefits of strength, resilience, durability, and accessibility that are attributable to concrete have made it a cornerstone of infrastructure development including roads and railways for transportation, dams for energy and irrigation, buildings for shelter, etc. Typical concretes are composed of different proportions of water, cement, sand, and aggregates, among which, cement is the hydraulic binder that holds the other components together, thereby making it an inevitable constituent. Cement is produced in over 150 countries with a current global demand of approximately 4.1 billion metric tonnes per year and expected to rise by 12–23% by 2050 [1], due to the economic buoyancy of several developing countries as well as the increased need for reconstructions due to internal displacements (especially in Sub-Saharan Africa, the Middle East, and Eastern European regions) arising from conflicts. In recent years, China has accounted for approximately 52% of the world's cement production (approximately 2.1 billion metric tonnes), followed by India at approximately 6.2% (approximately 381 million metric tonnes), then the USA with approximately 1.9% (approximately 95 million metric tonnes) [1]. Africa and Europe respectively contributed approximately 5% and 5.3% to the global cement production [2–4].

Despite the undeniable relevance and global accessibility of cement, its manufacturing process currently accounts for almost 8% of the global CO_2 emissions [3] owing to low resource efficiency, especially during the decarbonisation of limestone to produce calcium-rich clinker under high temperatures, with typical clinkerisation temperature reaching 1300–1450 °C in rotary kilns. It has been estimated that cement operations in general contribute immensely to environmental impacts, being accountable for 5–8% of anthropogenic greenhouse gas (GHG) emissions [5,6]. Approximately 50% of the CHG emissions from cement operations are directly linked to the chemical processing of the raw materials, while 40% are associated with the burning of fuel to power the process, electricity accounts for 5% and transportation accounts for the remaining 5% [2,3]. The culmination of these also results in high geogenic CO2 emissions [7,8]. Studies [4] have argued that if this emission rate continues, the global mean surface temperature by 2100

* Corresponding author.
E-mail address: akilu.kaltungo@manchester.ac.uk (A. Yunusa-Kaltungo).

https://doi.org/10.1016/j.conbuildmat.2024.136657
Received 12 December 2023; Received in revised form 18 April 2024; Accepted 13 May 2024
Available online 16 May 2024

could rise by as much as 2 °C to 4.8 °C when compared to the pre-industrial era. Furthermore, air emissions of sulphur oxides, nitrogen oxides, and particulate matter are additional sources of health concerns to humans and other living organisms [9,10].

To curb the high rates of carbon emission and energy-intensiveness of cement manufacturing processes, various optimisation alternatives have been explored in the past decades, especially related to equipment, processes, and raw materials [11–16]. Notable examples of equipment upgrades include the introduction of grate coolers as substitutes for traditional planetary coolers; replacement of tower preheaters with suspension preheaters or pre-calciners; replacement of horizontal ball mills with vertical roller mills and/or roller presses; replacement of electrostatic precipitators with baghouse filters and the gradual phasing out of long wet kilns [11–13]. With regards to raw materials, it is now common for cement plants to introduce supplementary cementitious materials (SCMs) such as pulverised fly ash, natural pozzolans (including clays, shale, and some forms of sedimentary rocks), silica fumes, blast furnace slag, fly ash, volcanic ash, or inert additives such as limestone to better optimise their clinker-to-cement ratios [11–14]. Though capital-intensive, the combined effects of these earlier initiatives have led to immense reductions in CO_2 emissions over the last three decades [17]. While these are very impressive accomplishments, unfortunately, they are still inadequate owing to the significance of the residual CO_2 emission rates, which in turn threatens the environmental sustainability of this crucial industry.

Based on these premises, research endeavours have been recently directed towards introducing new supplementary materials that can help reduce the overall embodied energy and CO_2 in concrete through reductions in the amount of cement required while at the same time maintaining/boosting strength. One of such proliferating class of materials is carbon-based nanoscale materials such as graphene, owing to their unique surface area and superior strengths. Several studies [18–20] have argued that graphene can enhance the mechanical properties of cement composites, owing to its peculiar ability to regulate cracks at nanoscales before they propagate to micro- and meso-scales [21–25]. More impressively, several studies have reported that the addition of minute proportions of graphene to cementitious materials could immensely enhance their functionality, thereby creating avenues for reducing the quantities of cementitious materials required, which could in turn boost sustainable development. For example, Bai et al. [26,27] reported that the addition of 0.1 wt% of graphene can enhance compressive strength by as much as 16%. Liu [28] also reported 14.9%, 23.6%, and 15.2% enhancements in 7-day compressive, flexural, and direct tensile strengths respectively, with 0.025 wt% graphene sheets. Similarly, the compressive and flexural strengths of cement composites that contained 0.06 wt% were reported to rise by 11.0% and 30.6% respectively, when compared with pure cement [29]. Ho [30] also highlighted that the 28-day compressive and tensile strengths of concrete respectively increased by 34.3% and 26.9% with the addition of 0.07 wt% graphene.

Previous studies [26–28] have vehemently reported very encouraging outcomes (especially concerning enhanced compressive strengths) because of the incorporation of graphene; however, the dispersion of graphene into cement composites continues to pose challenges that can potentially be addressed by optimising graphene dispersion. The established approaches for dispersing graphene in cement composites are through dry dispersion, wet dispersion with ultrasonication, and wet dispersion without ultrasonication [31]. The current dry dispersion regimes entail powder-to-powder (P2P) mixing of graphene and cement in a concrete mixer or high-speed shear mixer for extended periods. However, studies [31,32] have described this approach as ineffective due to the extended mixture residence times, lack of real-time control mechanisms for the mixing process, and the formation of slip planes. The wet dispersion of graphene without ultrasonication involves the use of mechanical stirring mechanisms to initially disperse graphene in water and superplasticiser, after which the graphene-water-plasticiser solution is mixed with dry cement. Similarly, this approach has been criticised because of the inability of the electrostatic repulsion forces generated by the superplasticiser to exfoliate monolayer of graphene from stacks of graphene, which in turn leads to poor dispersion and compromised mechanical performance [31]. In the ultrasonication-based wet dispersion of graphene, superplasticiser is incorporated to weaken the van der Waals force between graphene sheets to enhance dispersion into the water, after which the backbone of superplasticiser molecules absorbs on the surface of the graphene sheets [33–35]. More recently, the ultrasonication-based wet dispersion of graphene has been prioritised by most studies, owing to the impressive mechanical characteristics of the mortar and concrete samples that it can create [31]. For instance, it has been shown to enhance the compressive and flexural strengths of mortar [31,36] and concrete [37,38] samples by approximately 20% and 40% respectively, but the negative charges of the side chain of superplasticiser molecules have been shown to create electrostatic repulsion forces that lead to the opposition of graphene sheets [39,40]. Furthermore, the ultrasonication-based wet graphene dispersion approach requires a significant amount of energy to address the challenges of sonicated graphene flakes from restacking and re-agglomerating when dispersing concentrated graphene, thereby making the process very costly and unfriendly to the environment [41]. The required time (up to 5 hours) and mixing volume (mostly less than 5 l) makes it impractical for industrial applications.

To improve the cost-effectiveness of ultrasonication-based wet graphene dispersion by reducing the energy demand of the associated processes, a more recent study by Dung et al. [42] proposed the adoption of aqueous graphene, which is an intermediate product of the electrochemical exfoliation of graphene powder that primarily contains 80% and 20% of water and graphene powder respectively. The aqueous graphene generated from this process is then applied in paste form, without the need for extensive drying, thereby reducing environmental impacts and cost of processing while still enhancing dispersion. As impressive as the potential benefits of aqueous graphene are to overall energy and cost reduction, the amount of water (80%) required for its processing is still very significant especially if this approach is to be incorporated into the regular production of cement composites. There may also be a need for significant operational process modifications (especially the handling and drying of the additional moisture content) if aqueous graphene is to be integrated into the conventional cement manufacturing process, which may lead to an offset in its anticipated cost benefits as well as impede the realisation of sustainable development goals such as clean water and sanitation (SDG6); responsible consumption & production (SDG12); climate action (SDG13); and life below water (SDG14).

Therefore, the overarching aim of this study is to experimentally explore the viability of a low-cost, low-energy purpose designed, and built homogenisation approach for powder-to-powder (P2P) dispersion of graphene in cement. The P2P dispersion method could potentially produce a large batch of uniformly distributed graphene-cement mixture within a few minutes. The realisation of this aim is also linked to four closely aligned objectives, which are thoroughly addressed within different sections of the paper. Objective 1 will focus on the examination of P2P dispersion mechanisms that are available in practice and within the literature to understand their strengths and limitations, especially concerning the characteristics of powders handled (e.g., powder type, powder particle size, powder flowability, etc.) and energy-intensiveness of the process. Objective 2 will describe the design, mode of operation, and peculiarities of the proposed P2P graphene-cement dispersion mechanism. Objective 3 will be dedicated to experimentally testing the mechanical performance of the graphene-cement produced from the proposed P2P dispersion approach through the implementation of scanning electron microscopy (SEM) In Objective 4, an assessment of the large-scale deployment of the process will be conducted, including analyses of the least intrusive cement operation locations for incorporating the process, potential occupational safety & health (OSH) implications,

as well as the key variables to consider when modelling the costs associated with such integrations.

2. Overview of existing dry raw materials dispersion mechanisms in cement operations

The cement manufacturing process relies heavily on the homogenisation of different raw materials so that the uniformity indexes of the outputs at successive process stages can be optimised, thereby enhancing the likelihood of producing highly reactive cement composites at competitive prices. Homogenisation in a typical cement operation commences from the raw materials extraction and preparation stage, whereby the major constituents such as limestone, alumina, sand, and iron ore, extracted as boulders from the quarry, are initially fed into crushers primarily for size reduction. However, the rotary actions from such crushers create a secondary blending action before the outputs (also known as a raw mix) are carefully layered into stockpiles, whereby segregation occurs because of fine particles being deposited at the central parts of the pile, while the coarse materials occupy the surface and lower parts of the pile. A reclaimer rake then cuts across the face of individual layers of the stockpile to ensure a good representation of different constituents of the raw mix before drying, grinding, and milling in the raw mills to produce raw meals. Further homogenisation of the raw meal then occurs within the blending silos, before their introduction to the rotary kilns for pyro-processing and clinkerisation. The final stages of homogenisation within most cement operations occur within the cement mills when clinker and other additives (including gypsum and SCMs) are milled, and within the cement silos through aeration. Previously, wet process cement operations were highly desirable, owing to the ease with which high raw mix uniformity is realisable through slurry homogenisation. However, the wet and semi-wet processes are associated with very high heat consumption, especially when drying the slurry within the rotary kilns, which in turn triggered exploration into powder-to-powder (P2P) homogenisation approaches for raw mix within the fields of aerodynamics and pneumatics [41,42]. According to Pernenkil and Cooney [32], the dispersion of key components within a mixture is a function of segregation intensity while the magnitude of segregation reflects the correlation of the composition of such key constituents per unit of time (if homogenisation is continuous) or per unit space (if homogenisation process is conducted in batches). Therefore, the fundamental purpose of good P2P homogenisers is to minimise the magnitude and intensity of segregation between the different constituents of a mixture [43,44]. An earlier study by Lacey [45] has already demonstrated that even the best physical homogenisers can only be optimised to achieve random mixtures, as it is impracticable and too costly to achieve perfect mixtures due to challenges associated with creating the perfect balance between segregation intensity and magnitude.

The current study is based on the premise of a novel P2P homogenisation approach for graphene and cement powders, that would be capable of achieving a reasonably random mixture for enhanced reactivity of the resultant graphene-enhanced cement (Gr-CEM). Hence, it was useful to initially examine the strengths and limitations of the most popular P2P homogenisers within the literature and practice. Table 1 provides a summary of the operating principles for different P2P homogenisers as well as the characteristics of the powders handled especially particle size and flowability. Although the summary indicates that a wide range of powders with different sizes have been adequately homogenised via P2P mechanisms, there are at least three drawbacks with regard to the specific needs of Gr-CEM. Firstly, none of the existing approaches (either in theory or practice) has been used to handle large volumes of materials at nanoscales such as graphene. Secondly, most of the existing P2P homogenisers are dynamic in nature due to the incorporation of rotating components, which is detrimental to energy optimisation and maintenance costs. Thirdly, most of the existing homogenisers are designed for continuous operations which limits the operational flexibility of cement plants, especially during the current age of stringent market competition whereby manufacturers are aiming to segment their markets as much as possible. However, since only tiny quantities of graphene (usually $\leq$0.1% by weight) are required at any given time, a batch P2P homogeniser may be preferred to better optimise operational time and costs. Based on these premises, the proposed innovative P2P blending approach is a static pneumatically controlled batch homogeniser (SPCBH) and further details about its configuration are provided in Section 3.

Table 1
Summary of historical studies on P2P homogenisers and the main attributes of the materials handled.

Homogeniser Type	Powder			References
	Type	Attributes	Particle Size (μm)	
Rotating drum	Sand	Free flowing	355–420	[46,47]
	Limestone	Free flowing	40–200	[48,49]
	Dry powder	Free flowing	335	[50]
	Lignite	Free flowing	9600	[50]
	Zircon and coal		1700	[50]
	Rice and oats	Free flowing	2000	[50]
	Coal	Free flowing	500–20000	[50]
	Glass beads	Free flowing	3000	[50]
Rotating drum with double helical ribbon	Copper	Free flowing	10–85	[51,52]
Rotating drum with double auger	Silica flour	Cohesive	50	[32,53]
Rotating drum with bow-tie helical static	Coarse sand	Free flowing	700	[32,53]
Rotating drum with vibrating rotating paddle	Granular sugar	Free flowing	450	[32,53]
Rotating drum with horizontal double shaft	Aluminium hydroxide	Cohesive	27–71	[32,54]
Rotating drum with double concentric helical shaft	Silicon carbide	Free flowing	0.05–2.3	[32,54]
Rotating drum with ploughshare	Crushed maize	Free flowing	370	[32,55]
Static	Lucite	Free flowing	3175–5770	[56]

3. Research methodology

This section describes the main attributes of the proposed SPCBH and its mode of operation. Furthermore, the physical and chemical characteristics of the blended powders (i.e., graphene and cement) were also provided, especially particle sizes, specific surface area, and the percentages of main and trace constituents.

3.1. Description of the proposed SPCBH for P2P dispersion of graphene in cement

Within the last four decades, cement operations have witnessed significant advancements in the field of aerodynamics and pneumatics, especially regarding designs of material transport and homogenisation. However, irrespective of whether the traditional mixing chamber silos, air-merge or cone compartment silo design is adopted, a common denominator for their operations is the availability of semi-permeable

aeration units that direct air from compressors or blowers into the mixture for P2P fluidisation. In most existing designs, the aeration units deliver air to the mixture from the base of the silo to initially loosen the mixture and then reduce segregation via violent turbulent flow. Similarly, the simplified and energy-efficient P2P homogeniser used to generate the Gr-CEM employed here is a cylindrical vessel with four air-locked quadrants at the bottom. Primary mixing air is injected into the bottom of the cylinder via base quadrants to provide initial agitation, as well as to mitigate against dead material. Secondary air from two mini-scale root blowers was additionally introduced from multiple locations along the circumference of the cylinder to create violent turbulence to randomise the mixture. Owing to the very small graphene-to-cement ratio required for the experiment, a batch mixing approach is considered ideal as this will enable organisations that wish to adopt this approach to retain a variety of products, especially those products (e.g., Portland cement CemI 52.5 N and Portland cement 42.5 N) that are already popular to their most prominent client base. Each batch was operated for approximately six minutes. Fig. 1 depicts a schematic representation of the proposed P2P homogeniser for better clarity.

3.2. Raw materials preparation

In this study, Portland Cement (PC) CEMI 52.5 and CEMII 42.5 N, which are commercially available within the market. The main chemical components within both cement classes that facilitate the formation of C-S-H hydration products are CaO, SiO2, and Al2O3, although there are other minor elements as shown in Table 2. The particle size of cement powders is mainly within 1–10 μm with a typical surface area of 362 m^2/kg. The studies by Ferraris et al. [57], and that by Martínez-Alanis and López-Urías [58] provide details of the particle size distribution of typical Portland cement.

The graphene used in this study was of 20 μm diameter and its particle size distribution and the corresponding 2D geometries are shown in Fig. 2 and 3. More specifically, Fig. 3 shows a normalised, average of a 100-point Raman map, which was obtained by a Confocal Invia Qontor Raman. The graphene was pressed into a pellet then the Raman map was taken over the surface of the pellet. The transparency of the graphene platelets observed in the TEM analysis confirms that the PureGRAPH™ product range contains high levels of Few-Layer Graphene platelets. The typical number of layers for PureGRAPH™ 20 graphene product (i.e., 20 μm diameter type used in this study) is 10–15.

4. Experimental validation

To prove the concept and validate the uniform dispersion of graphene in cement materials, the microscopic analysis was used to observe the distribution of graphene in cement dust samples with quantification of graphene proportion by the post-imaging process. Flow table tests and compression tests were also carried out to measure the flowability and compressive strengths of the mortar pastes which used the conventional Ordinary Portland Cement (OPC) and Gr-CEM cement.

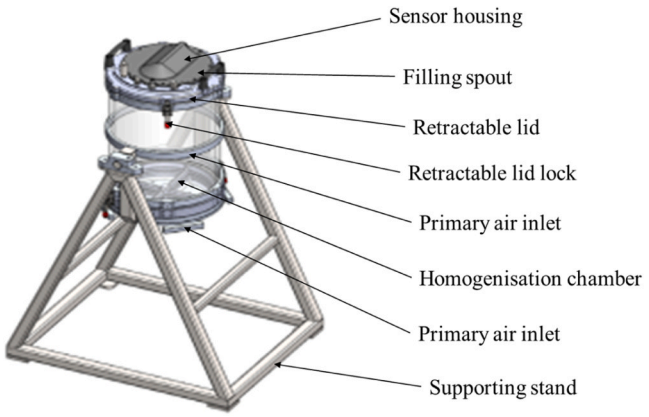

Fig. 1. Static pneumatically controlled batch homogeniser.

4.1. Microscopic analysis

Two samples with 1.00% and 0.02% of graphene were prepared for microscopic analysis. These samples were positioned between dual glass slides and observed using a Nikon Eclipse LV100N POL microscope, equipped with a 10x magnification objective. To ensure a standardized selection of observation areas, the filter elements were methodically folded twice, selecting four distinct areas from the central part of each fold for each sample, as shown in Figs. 4a and 4(b). Within each chosen area, nine discrete zones were systematically photographed using a Nikon DS-Fi2 camera, sequentially labelled from zone 1–9, as depicted in Fig. 4(c), ensuring an equitable distribution across the area under investigation. Optical imaging analyses were conducted using Avizo software (Thermo Fisher Scientific, USA), aiming to quantitatively assess the ratio of graphene and cement within the samples. A median filter (square 10) was used to reduce image noise. An interactive thresholding module was applied to the filtered image and the different materials were selected according to their grayscale. Graphene has the lowest reflectivity, followed by cement, and, hence, they can be discriminated (Fig. 5). The volume fraction module of the software was then utilised on the segmented images to ascertain the volumetric proportions of graphene and cement. The intensity threshold for graphene was incrementally adjusted (±1) to estimate measurement uncertainties. For instance, with an initial intensity range set between 0 and 3 for graphene, volume fractions were computed across the ranges of 0–3, 0–2, and 0–4, thereby yielding an average value and associated errors. According to these calculations, the 1% graphene sample manifested an average graphene content of 0.9 ± 0.1%, whereas the 0.02% graphene sample demonstrated a graphene composition of 0.04 ± 0.01% within the cement matrix, as summarised in Table 3. The results indicate two key messages: (a) OSH measures should be implemented to avoid the absorption of graphene during the processing of the graphene-cement mixture as graphene could leak out with cement from the fluidised bed; and (b) the dispersion of graphene is relatively uniform in cement across all the samples collected.

4.2. Mechanical properties and workability

Four different dosages of graphene were considered to validate the effects of different proportions of graphene, i.e., 0%, 0.02%, 0.04% and 0.06% (by mass of cement). Two types of cement were used: Portland cement CEM I 52.5 N and Portland cement CEM II 42.5 N, which were supplied by one of the largest cement manufacturers in the UK. The sand is ISO Standard sand (i.e., CEN EN 196–1 natural sand that is mostly siliceous and contains clean particles that are isometric and rounded in shape). The water/cement ratio and the sand/cement ratio are consistent across the specimens, as shown in Table 4. The Gr-CEM powder was mixed with sand for one minute before adding water. After mixing for two minutes, the mortar was cast in 50 mm cubic moulds. The casting samples were consolidated by a vibrating table and finished by a trowel. They were demoulded after 24 hours of casting and cured in water before testing.

The flow table tests were conducted before casting according to ASTM C230/C230M-21 [59]. The compression tests of the 50 mm cube were conducted to obtain the 7-day and 28-day strengths according to ASTM C109/C109M-20 [60]. Compressive strength tests were carried out by an Instron 350 kN machine operated at a loading rate of 0.4 MPa/s. The average value was calculated and reported based on three measurements. Table 5 compares the workability obtained from flow table tests between the control sample (CS), Gr0.02%, Gr0.04% and Gr0.06% samples. The results indicate that the incorporation of a tiny amount of graphene does not have clear effects on the flowability of the

Table 2
Typical chemical compositions of the cement samples used in this study.

Type of cement	Composition (%)										
	CaO	SiO_2	Al_2O_3	MgO	Fe_2O_3	K_2O	Na_2O	Free CaO	$EqNa_2O$	SO_3	Cl
CEMI 52.5	64.53	19.64	5.52	1.01	2.58	0.68	0.22	1.53	0.68	3.55	0.053
CEMII 42.5 N	63.94	19.55	5.41	1.14	2.86	0.65	0.27	2.08	0.54	3.5	0.058

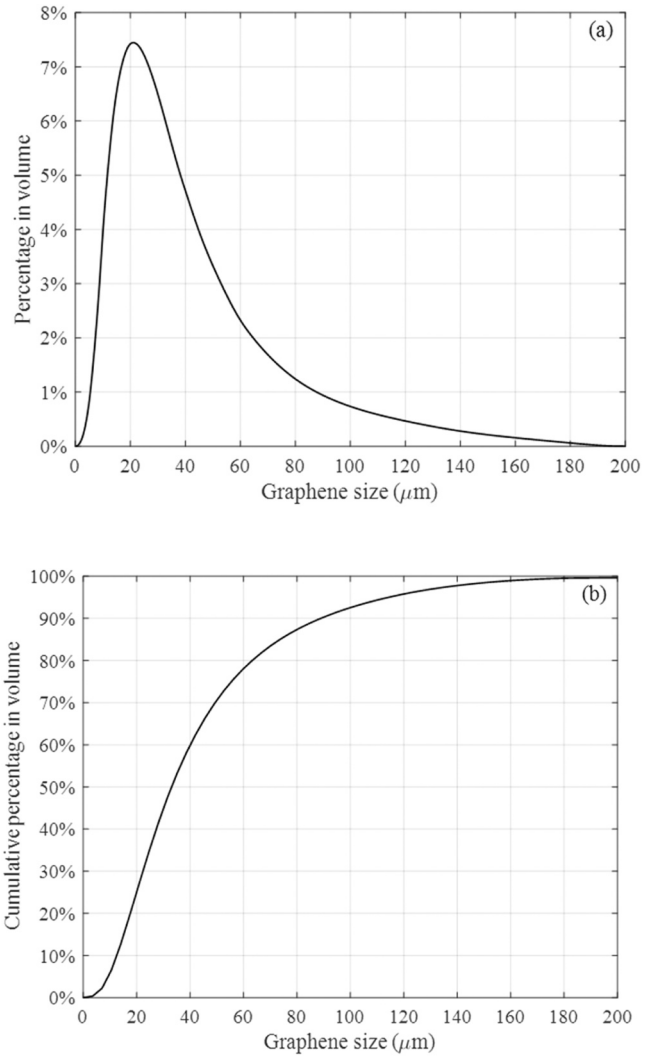

Fig. 2. Size distribution of graphene particles measured by Laser Diffraction Particle Size Analysis (a) percentage in volume (b) cumulative percentage in volume.

mortar paste; the differences in flowability of all samples are within 15%.

A comparison of the compressive strengths between the control sample and graphene-cement samples at 7 and 28 days is presented in Table 5. When using a small amount of graphene (<0.06%), the flowability of the mortar samples is not affected. The compressive strength of both CEM I and CEM II mortar samples improved when graphene was added. This could be attributed to the role of nucleation seeding of graphene to facilitate the hydration of cement particles and stimulate the formation of cement hydration products. Both CEM I and CEM II samples showed a consistent increase in compressive strengths after 7 and 28 days. Fig. 6 shows the effects of graphene dosage on the improved compressive strength of mortar samples. When as little as 0.02% graphene was utilized, the strength improvement achieved by mortar samples with CEM I cement without any additive was higher than those achieved by CEM II cement containing some additives. For both CEM I and CEM II samples, graphene content was optimal at 0.04%.

Furthermore, Fig. 7(a) and (b) present the heat flow and cumulative heat for all samples. The initial stage (up to 0.2 hours) for all samples involved dissolution and nucleation processes that began immediately after mixing with water. This was followed by an induction period with minimal heat release (0.5–3 hours for CEM I and 2 hours for CEM I + Gr 0.06%, CEM II, and CEM II + Gr 0.06% samples). During this period, dissolved ions accumulate to facilitate further nucleation and cement hydrate formation. The final stage (after 3 hours) is characterized by the acceleration and deceleration periods of hydration, with a corresponding high heat release due to nucleation, growth, and precipitation of reaction products. For CEM I, the inclusion of graphene in CEM I + Gr 0.06% sample resulted in several key observations. Significantly higher peaks were associated with both the dissolution/nucleation and acceleration/deceleration processes, as well as a shortened induction period compared to the CEM I sample. These results demonstrate an enhancement in hydration due to graphene introduction. This suggests that graphene within the pore space actively stimulates cement hydrate nucleation, facilitating the dissolution of cement particles at early stages, ultimately leading to higher cement hydrate nucleation and growth in the long term. The blend of ordinary Portland cement with other additives in CEM II samples improved their dissolution and nucleation compared to CEM I. Consequently, the role of graphene in enhancing these processes for CEM II was less pronounced than for CEM I. Nevertheless, the 0.06% graphene inclusion still resulted in the highest initial peak among all CEM II samples. Fig. 7(b), the cumulative heat plot, confirms a higher reaction degree for cement with graphene, especially for the CEM I sample. Additionally, the potential impact of graphene addition on the bulk densities of the resultant Gr-CEM I and Gr-CEM II via the proposed P2P method was also examined using two distinct experimental methods (i.e., Pycnometer/density cup and measuring cylinder methods) for cross-validation. For illustrative purposes, the experimentally determined bulk densities of CEM I (without graphene) and CEM II (without graphene) samples were compared with the bulk densities of Gr-CEM mixes with the highest dosage rates of graphene (i.e., CEM I + Gr 0.06% and CEM II + Gr 0.06%). Based on the examined samples, there were no significant differences in the resultant bulk densities as a result of the incorporation of graphene using the P2P method as shown in Table 6. The maximum difference between the bulk densities for all 4 samples is only 0.02 g/cm^3 for the Pycnometer/density cup method and only 0.04 g/cm^3 for the measuring cylinder method, which is all within the recommended ±5 accuracy levels.

5. Industrial viability analysis

Experimental results have already depicted significant enhancements in the compressive strength of the graphene-cement created from the proposed P2P homogenisation approach. However, the efficacy of any research endeavour is usually assessed based on how quickly and seamlessly the lessons learned from such theoretical and experimental investigations can be deployed to the industry for alleviating real-life challenges. Therefore, this section describes scenarios by which the P2P graphene-cement can be produced on a large scale within a cement manufacturing plant. Additionally, the possible enhancers and barriers associated with each scenario were highlighted to provide a holistic

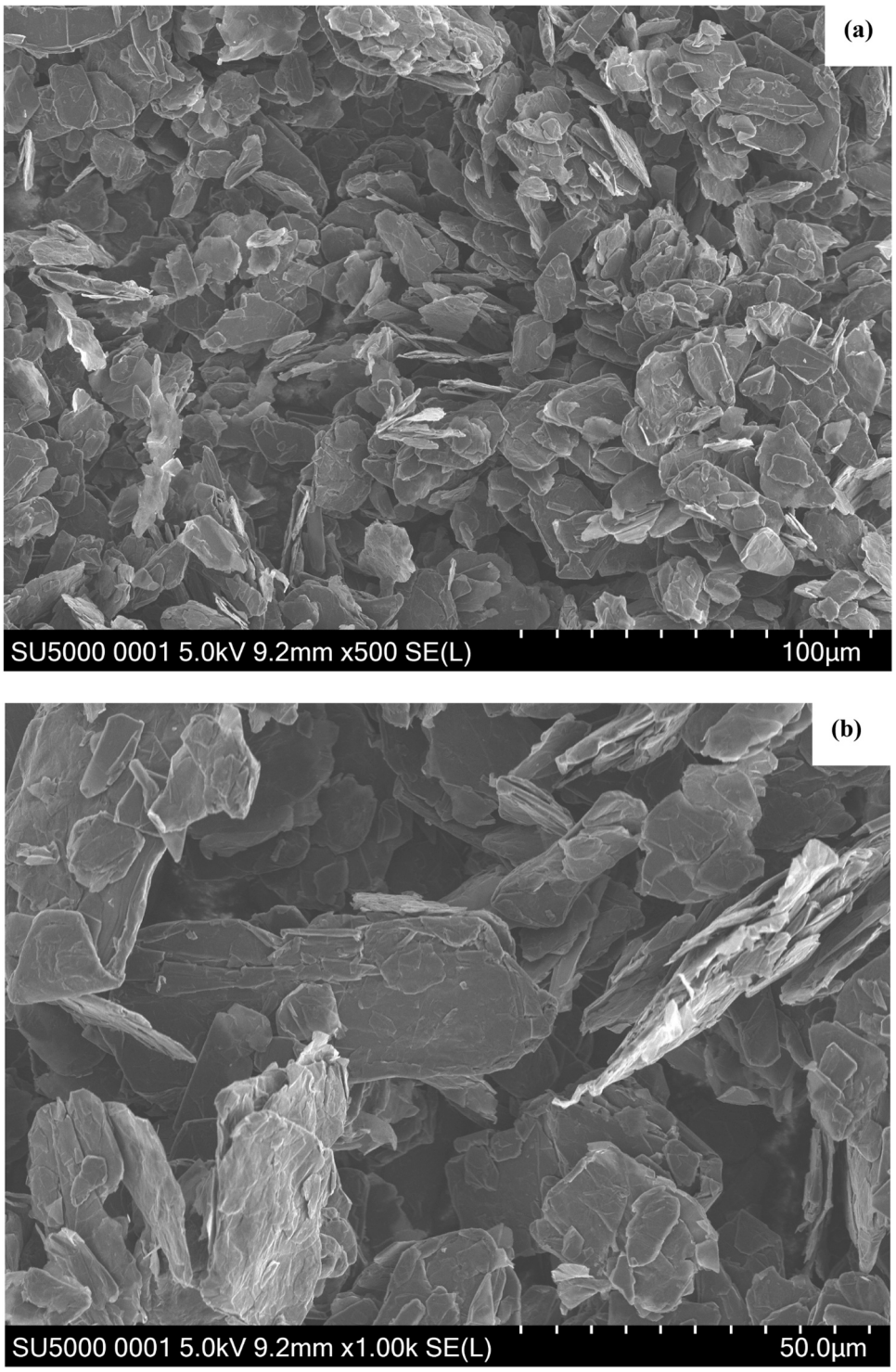

Fig. 3. 2D geometries of graphene particles in SEM images.

picture of the product's route to market.

5.1. Product handling and operational flexibility

Four P2P operational scenarios (OS1-OS4 in Fig. 8) were considered for large-scale industrial deployment within an all-integrated cement manufacturing process and in each scenario, implications on operational flexibility, occupational H&S and costs were examined. Fig. 8 is an abridged flow diagram for a cement manufacturing process, with particular emphasis on clinker (the hydraulic binder in cement compounds) production and grinding in the rotary kiln and cement ball mill respectively. In P2P operational scenario 1 (OS1), graphene will be injected into the cement manufacturing process via the cement mill inlet alongside other additives (e.g., gypsum and other SCMs) where it will be further pulverised and mixed with other materials before being transported to the cement storage silos via the cyclone separator, bag house or electrostatic precipitator, pneumatic pumps or other mechanical conveying systems and pipework. In terms of investment and operational requirements, this scenario is the path of least disruption to production setup because the required quantities of graphene can be easily

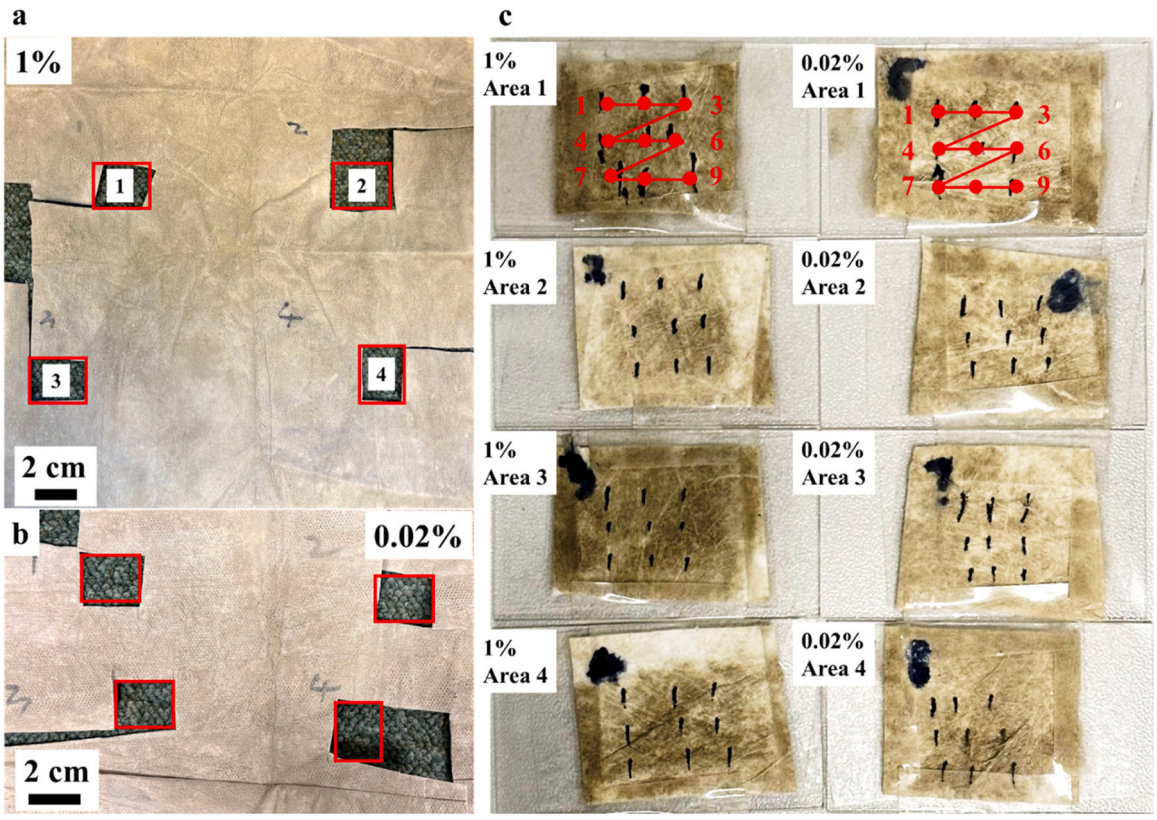

Fig. 4. Sample preparation. (a) 1.00% graphene sample and selection of four areas. (b) 0.02% graphene sample and selection of four areas. (c) The zones captured from studied areas in 1% and 0.02% sample. Nine zones evenly dispersed across a given area.

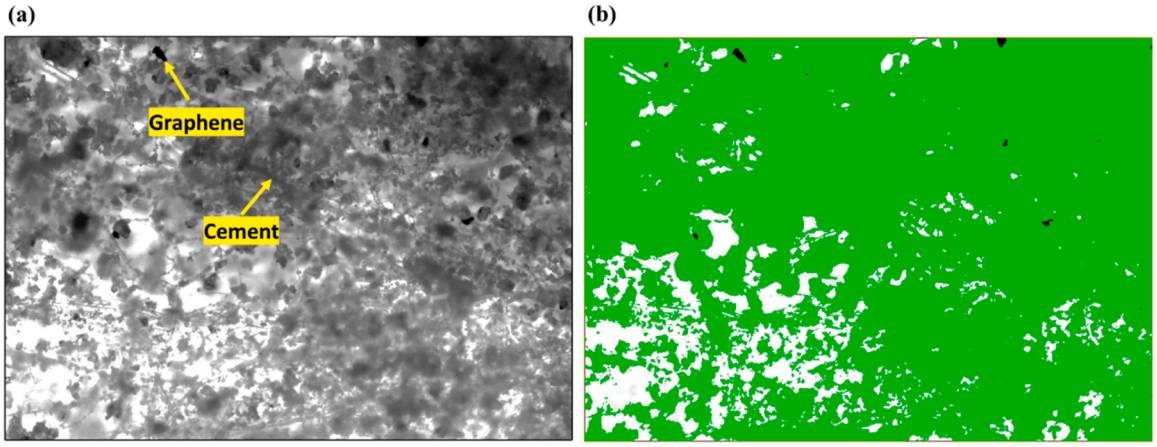

Fig. 5. Optical image analysis. (a) Optical image of graphene and cement. Image from area 4, zone 1, 0.02% sample. (b) Segmented graphene in black, cement in green and mask in white.

added with minimal physical modification to the operational layout of the cement plant, which could make it cheaper in the short term.

Despite the ease of dry graphene injection through OS1, it poses challenges to process control on several fronts. Firstly, it is impossible to control or guarantee the uniformity of graphene-cement mix through OS1, due to the one-pass air-swept nature of most cement grinding mills which could lead to the segregation of graphene particles. Secondly, OS1 has a long transmission path, which implies a higher possibility of graphene particles being trapped on intricate parts of intermediate process equipment along the pathway. Thirdly, OS1 has a higher risk profile because more people (e.g., cleaners, inspectors, maintainers, etc.) could be exposed to nanomaterials at the different intermediate process equipment. Fourthly, cement plants with a single cement storage silo are restricted to producing a single type of cement at every given instance, which in turn limits operational flexibility and product diversification. In P2P operational scenario 2 (OS2), graphene will be injected downstream of the cement mills via the cyclone separator to slightly minimise the transmission path and fewer contact surfaces between graphene injection and graphene-cement extraction points, thereby reducing graphene losses and the number of people exposed to nanomaterials. Despite the potential benefits of OS2, it would encounter some of the challenges associated with OS1, particularly the segregation of graphene due to limited residence time control mechanisms for the graphene-cement mix and poor product diversification. Furthermore, unlike in

Table 3
The quantification of percentage of graphene over cement in the studied samples.

1.00% graphene sample												
	Percentage of graphene over cement in the sample											
Zones	Area 1			Area 2			Area 3			Area 4		
	a	b	c	a	b	c	a	b	c	a	b	c
1	1.0	1.3	0.8	0.3	0.5	0.3	0.7	0.8	0.7	1.7	1.8	1.6
2	1.8	2.1	1.6	0.8	1.0	0.7	1.7	1.8	1.6	0.4	0.5	0.3
3	1.6	1.8	1.5	0.5	0.6	0.5	1.4	1.5	1.4	1.4	1.4	1.3
4	0.5	0.6	0.5	1.5	1.7	1.3	0.9	1.0	0.9	0.6	0.6	0.5
5	1.3	1.4	1.2	0.9	1.0	0.4	1.3	1.4	0.7	0.4	0.4	0.3
6	1.1	1.2	1.0	0.6	0.7	0.6	1.4	1.5	1.3	0.7	0.7	0.6
7	0.2	0.3	0.2	1.1	1.2	1.1	0.5	0.6	0.4	0.7	0.8	0.7
8	0.3	0.3	0.2	1.2	1.3	1.0	0.4	0.5	0.3	0.9	1.0	0.9
9	0.5	0.6	0.4	1.1	1.2	1.0	1.1	1.3	1.0	1.1	1.1	1.1
Average	0.9	1.1	0.8	0.9	1.0	0.8	1.0	1.1	0.9	0.9	0.9	0.8
The average value of all areas										**0.9**	**1.0**	**0.8**
0.02% graphene sample												
	Percentage of graphene over cement in the sample											
Zones	Area 1			Area 2			Area 3			Area 4		
	a	b	c	a	b	c	a	b	c	a	b	c
1	0.00	0.00	0.00	0.00	0.00	0.00	0.00	0.00	0.00	0.11	0.12	0.06
2	0.08	0.09	0.08	0.06	0.07	0.04	0.00	0.00	0.00	0.00	0.00	0.00
3	0.12	0.13	0.12	0.00	0.00	0.00	0.00	0.00	0.00	0.00	0.00	0.00
4	0.00	0.00	0.00	0.00	0.00	0.00	0.00	0.00	0.00	0.22	0.24	0.17
5	0.00	0.00	0.00	0.00	0.00	0.00	0.03	0.04	0.02	0.00	0.00	0.00
6	0.00	0.00	0.00	0.04	0.04	0.03	0.04	0.04	0.03	0.00	0.00	0.00
7	0.02	0.02	0.02	0.00	0.00	0.00	0.00	0.00	0.00	0.43	0.49	0.38
8	0.00	0.00	0.00	0.04	0.05	0.03	0.00	0.00	0.00	0.00	0.00	0.00
9	0.03	0.04	0.03	0.00	0.00	0.00	0.03	0.04	0.03	0.18	0.20	0.16
Average	0.03	0.03	0.03	0.01	0.02	0.01	0.01	0.01	0.01	0.10	0.12	0.09
The average value of all areas										**0.04**	**0.04**	**0.03**

Table 4
Mixture proportion of mortars and flow table test results.

Mixes	cement	Water	sand	Graphene	Flow table values (mm)
CEM I	1	0.44	1.94	0	200
CEM I + Gr 0.02%	1	0.44	1.94	0.0002	230
CEM I + Gr 0.04%	1	0.44	1.94	0.0004	224
CEM I + Gr 0.06%	1	0.44	1.94	0.0006	230
CEM II	1	0.44	1.94	0	210
CEM II + Gr 0.02%	1	0.44	1.94	0.0002	223
CEM II + Gr 0.04%	1	0.44	1.94	0.0002	225
CEM II + Gr 0.06%	1	0.44	1.94	0.0002	215

OS1 where graphene can be simply added alongside other additives through existing storage hoppers and feed systems, new air-tight feed chutes or spouts will need to be created on the cyclone for graphene injection.

To alleviate the operational limitations of OS1 and OS2, this study emphasises the adoption of OS3 whereby the novel purpose-designed and built low-energy homogeniser is connected in-line to the cement dispatch pipework after the cement storage silo, if the considered cement process is only furnished with a single silo thereby ensuring the retention of the existing proprietary product as well as the new graphene-cement. However, if a cement process has multiple storage silos, OS4 could be considered. OS4 is an option to install the low-carbon homogeniser before the silos, whereby different products (e.g., OPC and graphene-cement) can be fed into dedicated silos via diverter mechanisms. More importantly, graphene will be better dispersed in cement via OS3 and OS4 (as demonstrated by the results of the microscopic analysis shown in Fig. 5) since all the critical operations parameters (including residence time, airflow rate, air volume, speed, etc.) associated with the mixing process are much more controllable. The ability to control the residence time also implies that more randomised graphene-cement mixtures can be generated, which is crucial for reactivity (which determines the attainment of attributes such as enhanced strengths) and overall P2P blending efficiency. Although the implementation of OS3 and OS4 would require some initial capital expenditure (CAPEX), however, this could be offset by the potential savings on operational expenditure (OPEX) due to significantly low energy consumption, low

Table 5
Average value of compressive strengths of mortar samples.

Mixes	7-day compressive strength (MPa)					28-day compressive strength (MPa)				
	S1	S2	S3	Ave	SD	S1	S2	S3	Ave.	SD
CEM I	48.9	51.5	48.6	49.7	1.59	62.6	62.3	60.7	61.9	1.02
CEM I + Gr 0.02%	52.7	56.7	57.9	55.8	2.72	68.0	75.4	61.9	68.4	6.76
CEM I + Gr 0.04%	58.7	59.2	56.2	58.0	1.61	72.6	71.6	77.0	73.7	2.87
CEM I + Gr 0.06%	59.4	58.2	57.0	58.2	1.20	69.5	70.7	70.9	70.4	0.76
CEM II	39.1	37.7	40.0	38.9	1.16	49.6	51.6	51.9	51.0	1.25
CEM II + Gr 0.02%	40.3	38.8	38.1	39.0	1.12	51.4	55.8	50.0	52.4	3.03
CEM II + Gr 0.04%	47.9	46.5	48.3	47.6	0.95	62.4	61.0	60.6	61.3	0.95
CEM II + Gr 0.06%	45.3	46.8	47.0	46.4	0.93	60.6	64.0	63.8	62.8	1.91

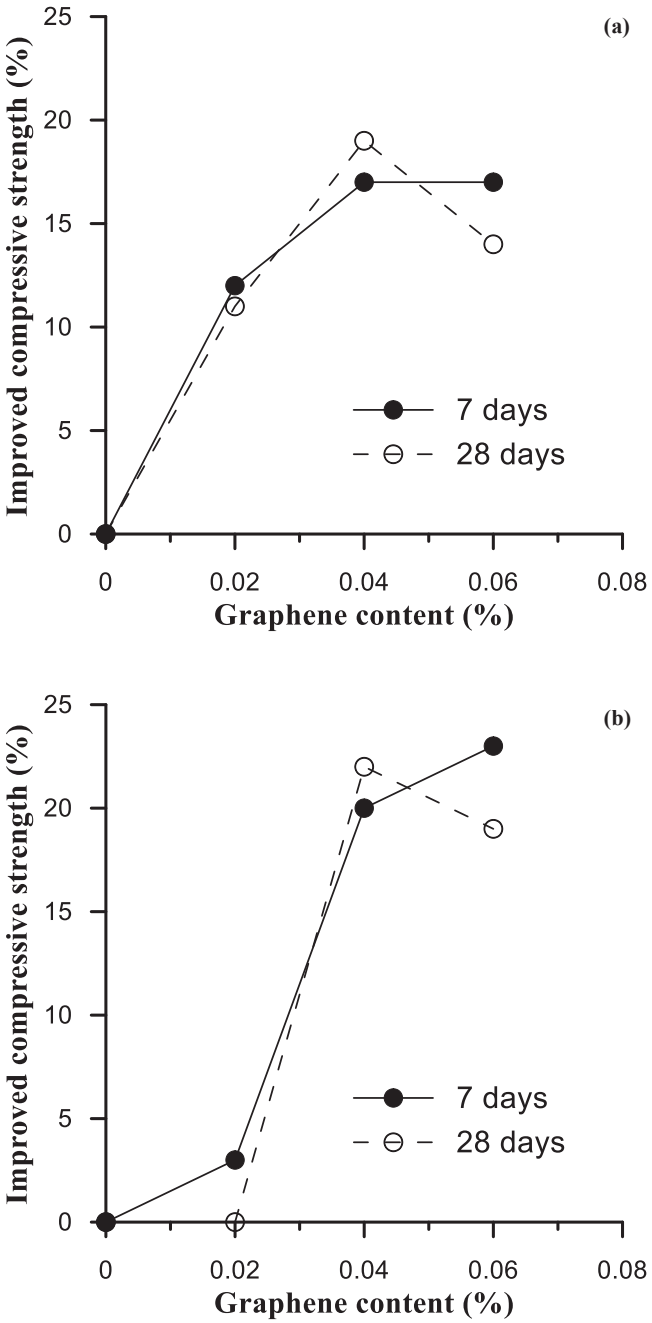

Fig. 6. Improvement in strengths due to the inclusion of graphene in (a) Portland cement CEM I 52.5 N and (b) Portland cement CEM II 42.5 N.

maintenance requirements due to zero moving parts, autonomous operation with no need for human interference, and diversity of products through operational flexibility.

5.2. Cost implications

Earlier sections have already demonstrated the mechanical characteristics of the proposed graphene-enhanced cement as well as the benefits of the low-energy homogeniser used for its production. This section discusses the cost implications of the industrial set-up and operation of the homogenisation system used for the P2P dispersion of graphene powder in cement. Cost considerations are key for gaining a comprehensive understanding of the viability of any business endeavour such as the introduction/incorporation of the homogenisation system into a cement production plant to inform business investment decision-

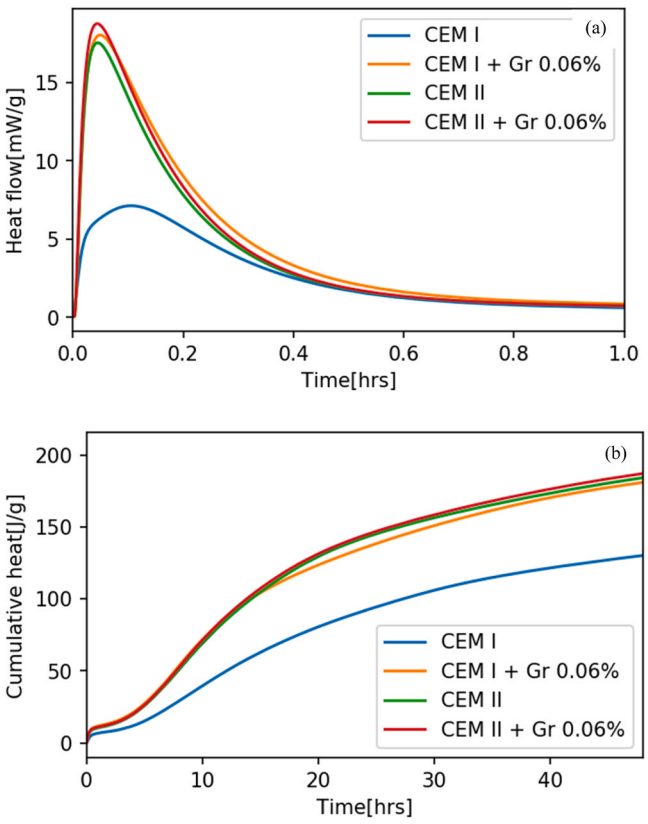

Fig. 7. Heat hydration for CEM I and CEM II samples with and without graphene at 0.06% dosage rate - (a) heat flow and (b) cumulative heat flow.

Table 6
Bulk densities of selected cement samples.

Sample Description	Density Measurement Technique	Sample Mass (g)	Sample Volume (cm3)	Density (g/cm3)
CEM I	Pycnometer/Density cup by Elcometer	57.1	57	1.00
	Measuring cylinder (500±5 ml In 20 °C)	268.7	256.3	1.05
CEM II	Pycnometer/Density cup by Elcometer	55.6	57	0.98
	Measuring cylinder (500±5 ml In 20 °C)	274.9	265	1.04
CEM I + Gr 0.06%	Pycnometer/Density cup by Elcometer	55.8	57	0.98
	Measuring cylinder (500±5 ml In 20 °C)	273.5	252.5	1.08
CEM II + Gr 0.06%	Pycnometer/Density cup by Elcometer	56.3	57	0.99
	Measuring cylinder (500±5 ml In 20 °C)	269.8	252.5	1.07

making. Consequently, a simplified mathematical model is presented here to serve as a guide to organisations to enable them to ascertain the cost components/constituents related to the initial set-up and operation of the homogenisation system. The cost of the system can be assessed in terms of the production cost per tonne of Gr-CEM ($C_{GR\text{-}CEM}$). The production cost/tonne of Gr-CEM would entail:

- Cost of the quantity of graphene in 1 tonne of Gr-CEM (C_G)
- Cost of the quantity of OPC in 1 tonne of Gr-CEM (C_{OPC})
- Cost of the homogenisation system per tonne of GR-CEM (C_{IDS}).

Considering the above variables, the cost per tonne of Gr-CEM ($C_{GR\text{-}}$

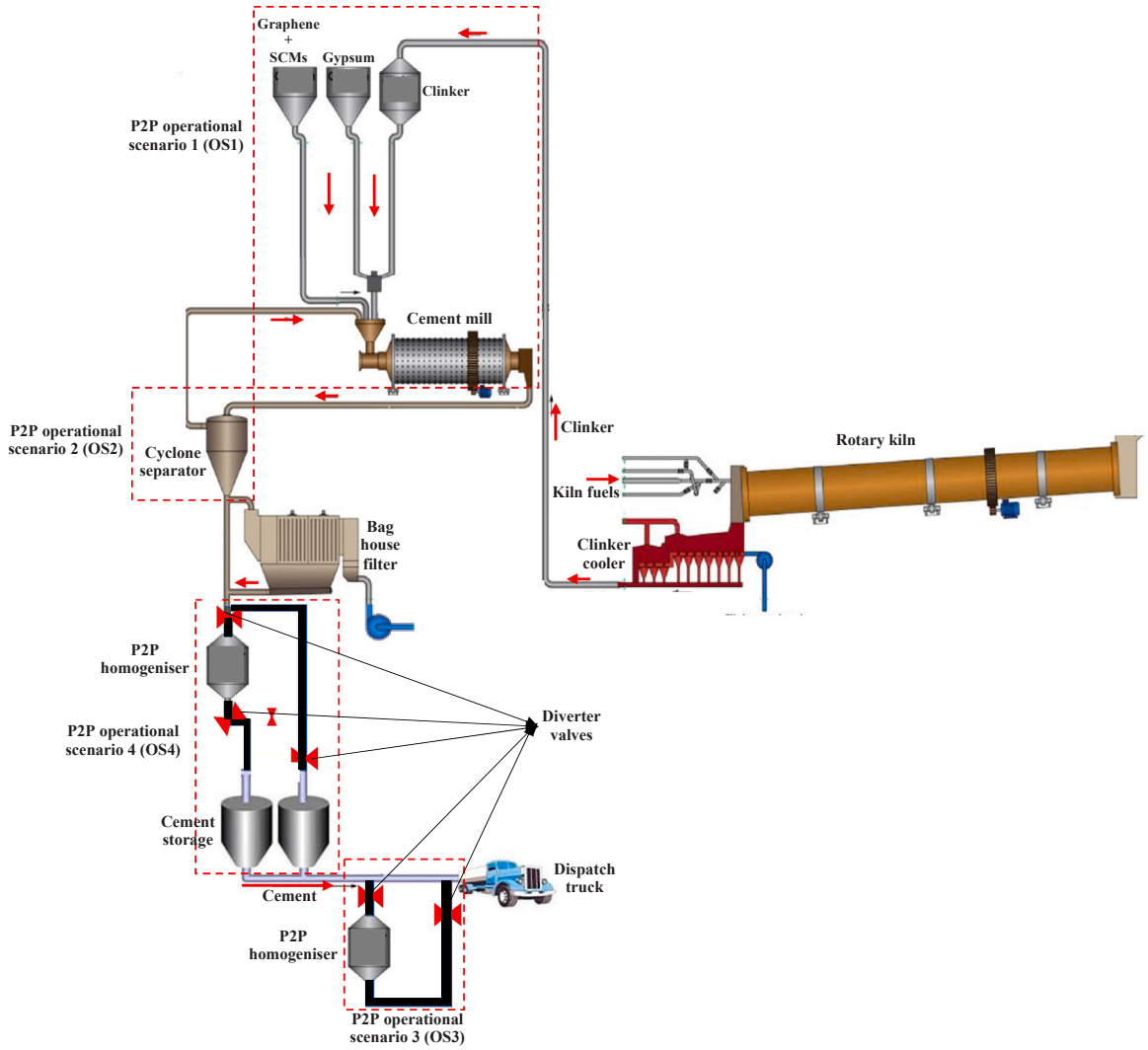

Fig. 8. Extract from an all-integrated cement process plant showing the different operational scenarios (adopted from Kogut et al. [61]).

$_{CEM}$) can be expressed as follows:

$$C_{GR\text{-}CEM} = C_G + C_{OPC} + C_{IDS} \quad (1)$$

While both the cost of the graphene (C_G) and the cement (C_{OPC}) can be obtained relatively easily from the existing business cost data/records, the cost of the homogenisation system per tonne of Gr-CEM (C_{IDS}) has to be estimated. C_{IDS} can be determined by estimating the cost per time (e.g., hourly) associated with using the homogenisation system (C_t) and then charging that cost per time against the time (T) (e.g., hours) taken to produce 1 tonne of Gr-CEM. Eq. 1 can therefore be rewritten as:

$$C_{GR\text{-}CEM} = C_G + C_{OPC} + (Ct * T) \quad (2)$$

A build-up of the estimated cost per time for the homogenisation system can be undertaken through an installation and operational life cost (IOLC) assessment approach. The IOLC will encapsulate: (a) initial installation (capital) cost (CAPEX) e.g., cost of design, fabrication, installation, testing and commissioning; and (b) operating cost (OPEX) e.g., energy cost, staff costs (including training to operate the system), and maintenance cost. It should be noted that the IOLC presented here can be easily converted to the life cycle cost (LCC) once information related to the end-of-life of the new GR-Cem become available. This is expressed by Eq. 3 below:

$$IOLC = Capex + Opex \quad (3)$$

Depending on the anticipated operational life of the system (expressed in number of years), the net present value (NPV) technique can be used to estimate the OPEX over the operational life as follows:

$$OPEX = \sum_{t=1}^{n} \frac{cost_t}{(1 + rate)^t} \quad (4)$$

Where 'cost' is the anticipated future operating cost at time 't', 'rate' is the discount rate, and 't' is the time (in years) of the cost.

Based on the annual operating time of the system (i.e., 'x' hours per year), the total operating time of the system over its operating life (i.e., 'n' years) can be estimated as follows:

$$Life\ operating\ time\ (LOT) = \text{'}x\text{'}\ hours\ per\ year * \text{'}n\text{'}\ years \quad (5)$$

Drawing on Eq. 3 and Eq. 5, the cost per time (e.g., hourly) associated with using the homogenisation system (C_t) can therefore be estimated as:

$$C_t = \frac{IOLC}{LOT} \quad (6)$$

6. Conclusion

The benefits of graphene addition to the performance of cement composites (especially mechanical strengths) are well-established

within existing literature. It is also known that the realisation of such strength benefits is highly dependent on how well graphene is dispersed within the cement composites, which has remained a research challenge. This is perhaps the reason why most of the existing studies on graphene-cement applications are based on the use of admixtures, superplasticisers, and ultrasonicators. These approaches have yielded some impressive results from product performance perspectives; however, they require significant amounts of energy and water, which may contradict the global plans for sustainable development goals such as clean water and sanitation (SDG6); responsible consumption & production (SDG12); climate action (SDG13); life below water (SDG14); and affordable and clean energy (SDG7). Therefore, this study proposes a novel purpose-built low-energy high-efficiency powder-to-powder (P2P) dispersion technique for graphene, cement and other SCMs. The proposed novel P2P homogenisation technique presents the potential to significantly enhance product performance, OSH, and plant operability through these summarised advantages:

6.1. Operational flexibility

The proposed P2P homogenisation approach offers a good degree of operational flexibility owing to its ability to be easily integrated into existing cement manufacturing systems at different locations, irrespective of whether the host cement plant is configured with single or multiple process lines and product storage silos. This implies that cement manufacturers are given the opportunity to deliver a wider range of products to existing and new customers, without necessarily compromising product quality or requiring significant capital (CAPEX) and operational expenditure (OPEX). For example, a cement plant can decide to retain existing proprietary products such as ordinary Portland cement (OPC) if still profitable, in addition to the new graphene-enhanced cement, thereby increasing their market share.

6.2. Product performance

The ability to control the residence times of mixtures is crucial for attaining good dispersion, which is highly correlated with strength enhancement and product throughput in cement operations. The results of the microscopic analysis indicate that the proposed P2P homogenisation approach offers the ability to adequately control the residence time of the graphene and cement mixture, which would be very challenging through any of the currently advocated injection approaches within existing literature. As opposed to most of the earlier studies that report strength enhancements based on samples created from CEM I which is of superior strengths due to higher composition of clinker, the experimental results of this study show that at least a 20% increase in compressive strengths was consistently realised from both CEM I and CEM II cement samples that are known for their lower strengths due to reduced clinker compositions. This implies that this approach offers immense opportunities to further substitute high-energy demanding clinker with low-energy supplementary materials such as limestone or other SCMs and still retain the required strength levels.

6.3. Responsible consumption of resources

In addition to its contribution to the preservation of rapidly depleting energy resources, the P2P homogenisation approach adopted here eliminates the need for other scarce natural resources, especially water during injection, which is crucial for the realisation of Sustainable Development Goals (SDGs) such as clean water and sanitation (SDG6), responsible consumption & production (SDG12), climate action (SDG13), and life below water (SDG14).

6.4. Industrial safety

The challenges of attaining good dispersion of graphene in cement are well documented within the existing body of knowledge. This is perhaps why most of the existing studies advocate the use of liquid-based approaches such as ultrasonication, where ultrasonic waves are used to irradiate the sample to create alternating high and low-pressure cycles. The most effective way of injecting the resultant admixture from this process into real-life cement operations is by feeding it into the cement mills alongside other supplementary materials for homogenisation. Besides the limitation of not being able to control the residence time of the mixture without compromising the throughput of the cement mills, this injection approach poses a higher OSH risk due to its long transmission path. To be more specific and depending on the layout of the particular cement plant, the resultant graphene-enhanced cement could pass through up to six distinct critical stages (including supplementary materials storages, cement mills, cyclone separators, bag filter units, cement storages, and cement despatch), thereby raising the risk of inhalation, ingestion, deposition on skin and other vital organs during routine inspections and maintenance activities. On the contrary, operational scenarios 3 and 4 (especially operational scenario 4) that are associated with the proposed homogenisation approach offer a significantly lower transmission path, since the resultant graphene-enhanced cement products will only pass through the despatch stage after injection. This approach minimises the risk of harm to employees and the environment significantly. If the concerned plants are bulk-loading plants that do not have an in-house packing stage for bagged products (such as that considered in the case study described here), the risk of harm to workers and the environment is even further reduced since the number of dedusting devices and possible dust emissions correspondingly reduces.

6.5. Cost-effectiveness

Most of the well-established fluidised bed homogenisers are associated with moving parts such as agitators, flap valves, screws, etc., and use high-pressure air supplies from compressors. From a maintenance point of view, the number of maintainable items and the eventual maintenance workload associated is also increased. Furthermore, the generation of compressed air continuously at 2–5 bar (as is the case with most traditional fluidised bed homogenisers) is energy-intensive and costly. However, the proposed homogeniser uses low-energy blowers (0.025 kW) to realise good air flow rates, offering a significantly cheaper and more environmentally friendly alternative. The shorter transmission path already discussed under industrial safety also implies that the possible impacts of the abrasiveness of carbon-based graphene are restricted to very few plant assets which could be crucial for reducing wear rates of assets and potential downtime reduction. Although the results presented here are all based on experiments, the study also provides a detailed step-by-step guide for estimating the economic viability of the proposed approach, to facilitate the decision-making process for cement plant owners during field-based implementation.

The powder-to-powder injection and homogenisation mechanism proposed in this study has cost-effectively generated graphene-enhanced cement with good degrees of dispersion, which has increased the compressive strengths of CEM I and CEM II cement samples by approximately 20%. However, the experimental investigations conducted here were based on only graphene and standard cement samples that contained fixed proportions of additives. Therefore, it would be useful for future studies to further investigate the robustness of the proposed homogeniser by considering its ability to facilitate the optimisation of cement-to-clinker ratios through the incorporation of higher proportions of other low-cost additives and/or supplementary cementitious materials, so that the embodied energy of cement products can be further lowered. It would also be useful to examine its ability to homogenise mixtures with a wider variation in particle sizes including clinkers with different free lime contents and size distributions.

CRediT authorship contribution statement

Raphael Tarpani: Writing – review & editing. **Alejandro Gallego-Schmid:** Writing – review & editing. **Lin Ma:** Writing – review & editing, Visualization, Validation, Methodology, Investigation, Formal analysis. **Jingyue Hao:** Writing – review & editing, Writing – original draft, Visualization, Methodology, Investigation, Formal analysis, Data curation. **Patrick Manu:** Writing – review & editing, Writing – original draft, Visualization, Validation, Methodology, Investigation, Formal analysis, Data curation. **Akilu Yunusa-Kaltungo:** Writing – review & editing, Writing – original draft, Visualization, Validation, Supervision, Resources, Project administration, Methodology, Investigation, Funding acquisition, Formal analysis, Data curation, Conceptualization. **Clara Cheung:** Writing – review & editing, Writing – original draft, Investigation. **Meini Su:** Writing – review & editing, Writing – original draft, Visualization, Validation, Methodology, Investigation, Formal analysis, Data curation.

Declaration of Competing Interest

The authors declare that they have no known competing financial interests or personal relationships that could have appeared to influence the work reported in this paper.

Data availability

Data will be made available on request.

Acknowledgement

The authors are immensely grateful to our industrial partners (Breedon Cement and First Graphene International Limited) for their support during this study.

References

[1] X. Li, D. Lepour, F. Heymann, F. Maréchal, Electrification and digitalization effects on sectoral energy demand and consumption: a prospective study towards 2050, Energy (2023 Jun 5) 127992.
[2] J. Farfan, M. Fasihi, C. Breyer, Trends in the global cement industry and opportunities for long-term sustainable CCU potential for Power-to-X, J. Clean. Prod. 217 (2019 Apr 20) 821–835.
[3] N. Tkachenko, K. Tang, M. McCarten, S. Reece, D. Kampmann, C. Hickey, M. Bayaraa, P. Foster, C. Layman, C. Rossi, K. Scott, Global database of cement production assets and upstream suppliers, Sci. Data 10 (1) (2023 Oct 13) 696.
[4] N. Kumar, D. Maiti, Long-run macroeconomic impact of climate change on total factor productivity—Evidence from emerging economies, Struct. Change Econ. Dyn. 68 (2024 Mar 1) 204–223.
[5] I. Junianto, Sunardi, D. Sumiarsa, The possibility of achieving zero CO2 emission in the Indonesian cement industry by 2050: a stakeholder system dynamic perspective, Sustainability 15 (7) (2023 Mar 31) 6085.
[6] A. Gallego-Schmid, H.M. Chen, M. Sharmina, J.M. Mendoza, Links between circular economy and climate change mitigation in the built environment, J. Clean. Prod. 260 (2020 Jul 1) 121115.
[7] R. Andersson, H. Stripple, T. Gustafsson, C. Ljungkrantz, Carbonation as a method to improve climate performance for cement based material, Cement and Concrete Research. 124 (2019) 105819.
[8] A.P. Gursel, E. Masanet, A. Horvath, A. Stadel, Life-cycle inventory analysis of concrete production: A critical review, Cement and Concrete Composites 51 (2014) 38–48.
[9] S.A. Miller, F.C. Moore, Climate and health damages from global concrete production, Nat. Clim. Change 10 (5) (2020 May) 439–443.
[10] E. Raffetti, M. Treccani, F. Donato, Cement plant emissions and health effects in the general population: a systematic review, Chemosphere 218 (2019 Mar 1) 211–222.
[11] A. Yunusa-Kaltungo, M.M. Kermani, A. Labib, Investigation of critical failures using root cause analysis methods: case study of ASH cement PLC, Eng. Fail. Anal. 73 (2017 Mar 1) 25–45.
[12] L.O. Iheukwumere-Esotu, A. Yunusa-Kaltungo, Knowledge criticality assessment and codification framework for major maintenance activities: a case study of cement rotary kiln plant, Sustainability 13 (9) (2021 Apr 21) 4619.
[13] A. Yunusa-Kaltungo, A. Labib, A hybrid of industrial maintenance decision making grids, Prod. Plan. Control 32 (5) (2021 Apr 4) 397–414.
[14] M. Toum Benchekroun, S. Zaki, M. Aboussaleh, Kiln predictive modelization for performance optimization, Int. J. Adv. Manuf. Technol. 127 (3) (2023 Jul) 1333–1339.
[15] R. Zhang, H. Yu, X. Wang, Research on modeling and optimization method of cement clinker calcination process based on EGPR model and steady state detection, IEEE Access (2023 Apr 19).
[16] M. Ren, T. Ma, C. Fang, X. Liu, C. Guo, S. Zhang, Z. Zhou, Y. Zhu, H. Dai, C. Huang, Negative emission technology is key to decarbonizing China's cement industry, Appl. Energy 329 (2023 Jan 1) 120254.
[17] W.R. Morrow III, A. Hasanbeigi, J. Sathaye, T. Xu, Assessment of energy efficiency improvement and CO2 emission reduction potentials in India's cement and iron & steel industries, J. Clean. Prod. 65 (2014 Feb 15) 131–141.
[18] D.R. Dreyer, S. Park, C.W. Bielawski, R.S. Ruoff, The chemistry of graphene oxide, Chem. Soc. Rev. *39* (2010) 228–240.
[19] L. Zhao, X. Guo, Y. Liu, C. Ge, L. Guo, X. Shu, J. Liu, Synergistic effects of silica nanoparticles/polycarboxylate superplasticizer modified graphene oxide on mechanical behavior and hydration process of cement composites, RSC Adv. 7 (27) (2017) 16688–16702.
[20] Z. Pan, L. He, L. Qiu, A.H. Korayem, G. Li, J.W. Zhu, F. Collins, D. Li, W.H. Duan, M.C. Wang, Mechanical properties and microstructure of a graphene oxide–cement composite, Cem. Concr. Compos. 58 (2015 Apr 1) 140–147.
[21] S. Musso, J.M. Tulliani, G. Ferro, A. Tagliaferro, Influence of carbon nanotubes structure on the mechanical behavior of cement composites, Compos. Sci. Technol. 69 (11-12) (2009 Sep 1) 1985–1990.
[22] A. Mohammed, J.G. Sanjayan, W.H. Duan, A. Nazari, Incorporating graphene oxide in cement composites: a study of transport properties, Constr. Build. Mater. 84 (2015 Jun 1) 341–347.
[23] C. Lu, Z. Lu, Z. Li, C.K. Leung, Effect of graphene oxide on the mechanical behavior of strain hardening cementitious composites, Constr. Build. Mater. 120 (2016 Sep 1) 457–464.
[24] W. Li, X. Li, S.J. Chen, G. Long, Y.M. Liu, W.H. Duan, Effects of nanoalumina and graphene oxide on early-age hydration and mechanical properties of cement paste, J. Mater. Civ. Eng. 29 (9) (2017 Sep 1) 04017087.
[25] W. Li, X. Li, S.J. Chen, Y.M. Liu, W.H. Duan, S.P. Shah, Effects of graphene oxide on early-age hydration and electrical resistivity of Portland cement paste, Constr. Build. Mater. 136 (2017 Apr 1) 506–514.
[26] S. Bai, L. Jiang, Y. Jiang, M. Jin, S. Jiang, D. Tao, Research on electrical conductivity of graphene/cement composites, Adv. Cem. Res. 32 (2) (2020 Feb) 45–52.
[27] S. Bai, L. Jiang, N. Xu, M. Jin, S. Jiang, Enhancement of mechanical and electrical properties of graphene/cement composite due to improved dispersion of graphene by addition of silica fume, Constr. Build. Mater. 164 (2018 Mar 10) 433–441.
[28] J. Liu, J. Fu, Y. Yang, C. Gu, Study on dispersion, mechanical and microstructure properties of cement paste incorporating graphene sheets, Constr. Build. Mater. 199 (2019 Feb 28), 1-1.
[29] W. Baomin, D. Shuang, Effect and mechanism of graphene nanoplatelets on hydration reaction, mechanical properties and microstructure of cement composites, Constr. Build. Mater. 228 (2019 Dec 20) 116720.
[30] V.D. Ho, C.T. Ng, C.J. Coghlan, A. Goodwin, C. Mc Guckin, T. Ozbakkaloglu, D. Losic, Electrochemically produced graphene with ultra large particles enhances mechanical properties of Portland cement mortar, Constr. Build. Mater. 234 (2020 Feb 20) 117403.
[31] Z. Lu, A. Hanif, G. Sun, R. Liang, P. Parthasarathy, Z. Li, Highly dispersed graphene oxide electrodeposited carbon fiber reinforced cement-based materials with enhanced mechanical properties, Cem. Concr. Compos. 87 (2018 Mar 1) 220–228.
[32] L. Pernenkil, C.L. Cooney, A review on the continuous blending of powders, Chem. Eng. Sci. 61 (2) (2006 Jan 1) 720–742.
[33] X. Li, Z. Lu, S. Chuah, W. Li, Y. Liu, W.H. Duan, Z. Li, Effects of graphene oxide aggregates on hydration degree, sorptivity, and tensile splitting strength of cement paste, Compos. Part A: Appl. Sci. Manuf. 1 (100) (2017 Sep) 1–8.
[34] H. Qin, W. Wei, Y.H. Hu, Synergistic effect of graphene-oxide-doping and microwave-curing on mechanical strength of cement, J. Phys. Chem. Solids 103 (2017 Apr 1) 67–72.
[35] Y.L. Zhong, Z. Tian, G.P. Simon, D. Li, Scalable production of graphene via wet chemistry: progress and challenges, Mater. Today 18 (2) (2015 Mar 1) 73–78.
[36] L. Göbel, C. Bos, R. Schwaiger, A. Flohr, A. Osburg, Micromechanics-based investigation of the elastic properties of polymer-modified cementitious materials using nanoindentation and semi-analytical modeling, Cem. Concr. Compos. 88 (2018 Apr 1) 100–114.
[37] K.A. Rod, M.T. Nguyen, M. Elbakhshwan, S. Gills, B. Kutchko, T. Varga, A. M. Mckinney, T.J. Roosendaal, M.I. Childers, C. Zhao, Y.C. Chen-Wiegart, Insights into the physical and chemical properties of a cement-polymer composite developed for geothermal wellbore applications, Cem. Concr. Compos. 97 (2019 Mar 1) 279–287.
[38] J.A. Rosewitz, H.A. Choshali, N. Rahbar, Bioinspired design of architected cement-polymer composites, Cem. Concr. Compos. 96 (2019 Feb 1) 252–265.
[39] A.B. Bourlinos, V. Georgakilas, R. Zboril, T.A. Steriotis, A.K. Stubos, C. Trapalis, Aqueous-phase exfoliation of graphite in the presence of polyvinylpyrrolidone for the production of water-soluble graphenes, Solid State Commun. 149 (47-48) (2009 Dec 1) 2172–2176.
[40] A.S. Wajid, S. Das, F. Irin, H.T. Ahmed, J.L. Shelburne, D. Parviz, R.J. Fullerton, A. F. Jankowski, R.C. Hedden, M.J. Green, Polymer-stabilized graphene dispersions at high concentrations in organic solvents for composite production, Carbon 50 (2) (2012 Feb 1) 526–534.
[41] E. Knapen, D. Van Gemert, Cement hydration and microstructure formation in the presence of water-soluble polymers, Cem. Concr. Res. 39 (1) (2009 Jan 1) 6–13.
[42] N.T. Dung, M. Su, M. Watson, Y. Wang, Effects of using aqueous graphene on behavior and mechanical performance of cement-based composites, Constr. Build. Mater. 368 (2023 Mar 3) 130466.

[43] D. Tsamatsoulis, Modelling and simulation of raw material blending process in cement raw mix milling installations, Can. J. Chem. Eng. 92 (11) (2014 Nov) 1882–1894.
[44] J.E. Bond, R. Coursaux, R.L. Worthington, Blending systems and control technologies for cement raw materials, IEEE Ind. Appl. Mag. 6 (6) (2000 Nov) 49–59.
[45] P.M.C. Lacey, The mixing of solids particles, Trans. Inst. Chem. Eng. 21 (1943) 53.
[46] J.C. Williams, M.A. Rahman, Prediction of the performance of continuous mixers for particulate solids using residence time distributions Part I. Theoretical, Powder Technol. 5 (2) (1972 Jan 1) 87–92.
[47] J.C. Williams, M.A. Rahman, Prediction of the performance of continuous mixers for particulate solids using residence time distributions: Part II. Experimental, Powder Technol. 5 (5) (1972 Apr 1) 307–316.
[48] W. Müller, Untersuchungen zur pulvermischung, Chem. Ing. Tech. 39 (14) (1967 Jul 26) 851–858.
[49] W. Müller, H. Rumpf, Das mischen von pulvern in mischern mit axialer mischbewegung, Chem. Ing. Tech. 39 (5-6) (1967 Mar 20) 365–373.
[50] R.G. Sherritt, J. Chaouki, A.K. Mehrotra, L.A. Behie, Axial dispersion in the three-dimensional mixing of particles in a rotating drum reactor, Chem. Eng. Sci. 58 (2) (2003 Jan 1) 401–415.
[51] K.R. Poole, Mixing powders to fine-scale homogeneity studies of batch mixing, Trans. Instn Chem. Engrs 42 (1964) T305–T315.
[52] K.R. Poole, R.F. Taylor, G.P. Wall, Mixing powders to fine-scale homogeneity-studies of continuous mixing, Trans. Instn Chem. Engrs. 43 (9) (1965 Jan 1) T261.
[53] C.F. Harwood, K. Walanski, E. Luebcke, C. Swanstrom, The performance of continuous mixers for dry powders, Powder Technol. 11 (3) (1975 May 1) 289–296.
[54] R. Weinekötter, L. Reh, Continuous mixing of fine particles, Part. Part. Syst. Charact. 12 (1) (1995 Feb) 46–53.
[55] Merz A., Holtzmüller R. Radionucleide investigations into the influence of the mixer chamber geometry on the mass transport in a continuous ploughshare mixer. InProceedings of the second Symposium on mixing of particulate solids 1981 (No. 65, p. S1).
[56] S.J. Chen, L.T. Fan, C.A. Watson, Mixing of solid particles in motionless mixer-axial-dispersed plug-flow model, Ind. Eng. Chem. Process Des. Dev. 12 (1) (1973 Jan) 42–47.
[57] C.F. Ferraris, V.A. Hackley, A.I. Aviles, Measurement of particle size distribution in Portland cement powder: analysis of ASTM round robin studies, Cem., Concr., Aggreg. 26 (2) (2024). CCA11920.
[58] M. Martínez-Alanis, F. López-Urías, Cement pastes and mortars containing nitrogen-doped and oxygen-functionalized multiwalled carbon nanotubes, J. Mater. 2016 (2) (2016 Feb 28) 1–16, 6209192.
[59] American Society for Testing and Materials. Standard specification for flow table for use in test of hydraulic cement (ASTM C230/C230M-21). Book of Standards volume 04.01, ICS code: 91.100.10. DOI: 10.1520/C0230M-21.
[60] American Society for Testing and Materials. Standard test method for compressive strength of hydraulic cement mortars (using 2-in. or [50-mm] cube specimens). Book of Standards volume 04.01, ICS code: 91.100.10. DOI: 10.1520/C0109M-20.
[61] K. Kogut, J. Gorecki, P. Burmistrz, Opportunities for reducing mercury emissions in the cement industry, J. Clean. Prod. 293 (2021 Apr 15) 126053.